ISSN 1674-1056
http://cpb.iphy.ac.cn
http://iopscience.iop.org/cpb
中国物理 B
Chinese Physics
中国物理 Chinese Physics B

Cavity-induced ATS effect on a superconducting Xmon qubit

Xueyi Guo(郭学仪), Hui Deng(邓辉), Jianghao Ding(丁江浩), Hekang Li(李贺康), Pengtao Song(宋鹏涛), Zhan Wang(王战), Luhong Su(苏鹭红), Yanjun Liu(刘彦军), Zhongcheng Xiang(相忠诚), Jie Li(李洁), Yirong Jin(金贻荣), Yuxi Liu(刘玉玺), Dongning Zheng(郑东宁)

Citation: Chin. Phys. B . 2018, 27(8): 084202. **doi:** 10.1088/1674-1056/27/8/084202

Journal homepage: http://cpb.iphy.ac.cn; http://iopscience.iop.org/cpb

What follows is a list of articles you may be interested in

Bridge-free fabrication process for Al/AlO$_x$/Al Josephson junctions

Ke Zhang(张珂), Meng-Meng Li(李蒙蒙), Qiang Liu(刘强), Hai-Feng Yu(于海峰), Yang Yu(于扬)
Chin. Phys. B . 2017, 26(7): 078501. **doi:** 10.1088/1674-1056/26/7/078501

Autler-Townes spectroscopy of high-lying state by phase conjugate six-wave mixing

Jin-Hai Bai(白金海), Jian-Jun Li(李建军), Ling-An Wu(吴令安), Pan-Ming Fu(傅盘铭), Ru-Quan Wang(王如泉), Zhan-Chun Zuo(左战春)
Chin. Phys. B . 2017, 26(4): 044204. **doi:** 10.1088/1674-1056/26/4/044204

Crossover between electromagnetically induced transparency and Autler-Townes splitting with dispersion

Lu Xiao-Gang, Miao Xing-Xu, Bai Jin-Hai, Yuan Yuan, Wu Ling-An, Fu Pan-Ming, Wang Ru-Quan, Zuo Zhan-Chun
Chin. Phys. B . 2015, 24(9): 094204. **doi:** 10.1088/1674-1056/24/9/094204

Relationship between electromagnetically-induced transparency and Autler–Townes splitting in a Doppler-broadened system

Pei Li-Ya, Niu Jin-Yan, Wang Ru-Quan, Qu Yi-Zhi, Zuo Zhan-Chun, Wu Ling-An, Fu Pan-Ming
Chin. Phys. B . 2015, 24(7): 074203. **doi:** 10.1088/1674-1056/24/7/074203

The difference in noise property between the Autler–Townes splitting medium and the electromagnetically induced transparent medium

Li Zhong-Hua,Li Yuan,Dou Ya-Fang,Zhang Jun-Xiang
Chin. Phys. B . 2012, 21(3): 034204. **doi:** 10.1088/1674-1056/21/3/034204

Cavity-induced ATS effect on a superconducting Xmon qubit*

Xueyi Guo(郭学仪)[1,2], Hui Deng(邓辉)[1], Jianghao Ding(丁江浩)[3], Hekang Li(李贺康)[1,2], Pengtao Song(宋鹏涛)[1,2], Zhan Wang(王战)[1,2], Luhong Su(苏鹭红)[1,2], Yanjun Liu(刘彦军)[1], Zhongcheng Xiang(相忠诚)[1], Jie Li(李洁)[1], Yirong Jin(金贻荣)[1], Yuxi Liu(刘玉玺)[3,4], and Dongning Zheng(郑东宁)[1,2,†]

[1] *Institute of Physics, Chinese Academy of Sciences, Beijing* 100190, *China*
[2] *School of Physical Sciences, University of Chinese Academy of Sciences, Beijing* 100049, *China*
[3] *Institute of Microelectronics, Tsinghua University, Beijing* 100084, *China*
[4] *Tsinghua National Laboratory for Information Science and Technology (TNList), Beijing* 100084, *China*

(Received 25 April 2018; revised manuscript received 18 May 2018; published online 10 July 2018)

We couple a ladder-type three-level superconducting artificial atom to a cavity. Adjusting the artificial atom to make the cavity be resonant with the two upper levels, we then probe the lower two levels of the artificial atom. When driving the cavity to a coherent state, the probe spectrum shows energy level splitting induced by the quantized electromagnetic field in the cavity. This splitting size is related to the coupling strength between the cavity and the artificial atom and, thus, is fixed after the sample is fabricated. This is in contrast to the classical Autler–Townes splitting of a three-level system in which the splitting is proportional to the driving amplitude, which can be continuously changed. Our experiment results show the difference between the classical microwave driving field and the quantum field of the cavity.

Keywords: superconducting qubit, circuit QED, Autler–Townes splitting

PACS: 42.50.Gy, 85.25.Cp **DOI:** 10.1088/1674-1056/27/8/084202

1. Introduction

When a multi-level quantum system interacts with an electromagnetic field, intriguing phenomena could appear, for example, electromagnetic-induced transparency (EIT).[1–9] In broad terms, EIT refers to the elimination/reduction of resonant absorption for propagating electromagnetic waves, when a strong driving field is applied to other atomic transitions, for example, three-level systems. This can create a transparency window for the propagating electromagnetic waves. There are, however, two types of underlying mechanisms associated with this phenomenon. The first one is the destructive interference between the two excitation pathways that creates a transparency window for one of the driving fields. Transparency due to this mechanism is called, in specific terms, EIT. Another one is related to Autler–Townes splitting (ATS), i.e., due to the energy level splitting by the strong driving field.[10,11] In ATS, a strong electromagnetic field is applied to drive, usually, the two upper levels of the three-level system while probing the two other levels. If the driving field is strong enough, the probe spectrum shows energy level splitting, and the splitting size is proportional to the driving field amplitude. It has been shown that EIT and ATS are closely related to each other and, for a given three-level system, there could be continuous transformation from EIT to ATS depending on the system parameters such as relaxation times between relevant levels.[12] These two effects have been investigated extensively and are regarded as useful techniques in building quantum networks.[13] Over the past decade, with the Josephson junction based superconducting circuits, which are also known as artificial atoms, these effects have been restudied and reproduced.[12–24]

In both EIT and ATS, the driving field is in the classical regime. In the quantum regime, the electromagnetic field is treated quantum mechanically and the field is quantized. The quantized field in a cavity with few photons or even zero photon could result ATS or EIT, the vacuum induced transparency has been studied in atomic systems.[25] However, due to the small dipole interaction, the coupling strength between nature atoms and quantized field is weak. Very recently, the vacuum or few photons induced energy level splitting and transparency have been theoretically analyzed in Ref. [26]. Also, an experimental study has been reported for a system that includes a superconducting flux qubit coupled to a superconducting coplanar wave-guide resonator.[27] Owing to the strong coupling between the superconducting flux qubit and the quantized field, the experiment shows vacuum induced ATS. However, in these two works, the system investigated is a Λ-type three-level sys-

*Project supported by the Science Funds from the Ministry of Science and Technology of China (Grant Nos. 2014CB921401, 2017YFA0304300, 2014CB921202, and 2016YFA0300601), the National Natural Science Foundation of China (Grant No. 11674376), and the Strategic Priority Research Program of the Chinese Academy of Sciences (Grant No. XDB07010300).

†Corresponding author. E-mail: dzheng@iphy.ac.cn

© 2018 Chinese Physical Society and IOP Publishing Ltd

tem. In this work, we investigated the vacuum induced ATS effect for a ladder-type system using an Xmon type superconducting qubit, which works as a three-level system (3LS).[28] Its lowest three levels are labeled as $|g\rangle$, $|e\rangle$, and $|f\rangle$. We replace the strong driving for the two upper levels with a resonantly coupled cavity. When there is one photon inside the cavity, similar to the classical ATS effect, it causes resonant splitting of the energy level. However, this energy level splitting induced by a vacuum is fixed by the coupling strength between the cavity and the three-level system, which is different from the classical ATS effect. When the coupling between the cavity and the three-level system is in a dispersive regime, the coherent state of the cavity causes a photon-number splitting spectrum, which has been shown in Ref. [23]. A single photon in a cavity corresponds to only one peak on the photon-number splitting spectrum. In Ref. [23], the authors also studied the classical ATS effect of a three level system formed by $|g1\rangle$ $|e0\rangle$ $|e1\rangle$ of the dispersively coupled system. Notice that this ATS effect is also the classical ATS effect, which is induced by resonantly driving between $|e0\rangle \leftrightarrow |e1\rangle$, and probes the energy level splitting by applying a probe wave between $|g1\rangle \leftrightarrow |e1\rangle$. Their results show, as the driving amplitude increases, the splitting increases too.

2. Experiment

The sample used in this study is an Xmon type qubit capacitively coupled to a $\lambda/4$ coplanar waveguide (CPW) resonator. The qubit is also coupled to a CPW transmission line from which the microwave photon transmission properties are measured. The transmitted microwave interacts with the qubit and an absorption peak would appear when the transmitted microwave is in resonance with the energy level spacing of the Xmon qubit. Hence, one can detect the qubit energy level by measuring the transmitted microwave spectrum.

An optical micrograph of the sample is shown in Fig. 1(a). The red part is the Xmon qubit, which works as our ladder-type three-level quantum system.[28,29] It can be treated as a nonlinear LC resonator, in which the two Josephson junctions form into DC-SQUID, shown in the inset of Fig. 1(a), and work as an adjustable nonlinear inductance. The energy level can be controlled by applying a DC bias through the Z control line. The green part is the $\lambda/4$ coplanar waveguide resonator.

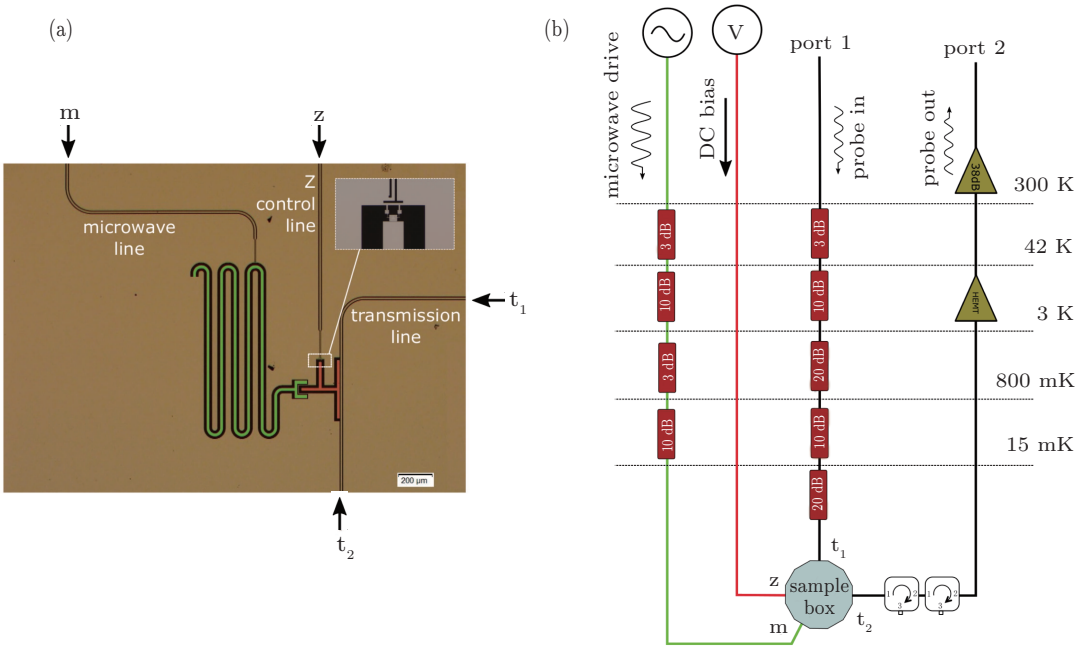


Fig. 1. (color online) (a) Optical micrograph of the sample. The red part is the Xmon qubit in which a DC-SQUID, shown in the inset, functions as a nonlinear inductor. The Z control line is inductively coupled to the DC-SQUID, and can be used to adjust the energy level of the Xmon. The green part is a $\lambda/4$ coplanar waveguide resonator, which can be driven by the microwave field applied through the microwave line. The resonator and the Xmon are capacitively coupled to each other. The Xmon is also coupled to the transmission line. (b) Schematic diagram of the experimental setup. The sample is packaged inside an aluminum alloy sample box that is mounted on the mixing chamber stage of a dilution refrigerator. The green line is used for applying a microwave field to drive the $\lambda/4$ coplanar waveguide resonator. The red line is used for adjusting the energy level of the Xmon. The black line is connected to the transmission line used for detection of the probe signal. Ports 1 and 2 are connected to a vector network analyzer.

The sample was fabricated using a process involving electron-beam-lithography (EBL) and double-angle evaporation. In brief, a 100-nm thick Al layer was firstly deposited on a 10 mm $\times$ 10 mm sapphire substrate by means of electron-beam evaporation, followed by EBL and wet etching to produce large structures such as microwave coplanar-waveguide resonators/transmission lines, capacitors of the Xmon qubit, and electron leads. The EBL resist used was ZEP520 and the

wet etching process was carried out using Aluminum Etchant Type A. In the next step, the Josephson junctions of qubits were fabricated using the double-angle evaporation process. In this step, the under cut structure was created using a PMMA–MMA double layer EBL resist following a process similar to that reported in Ref. [30]. During the evaporation, the bottom electrode was about 30-nm thick while the top electrode was about 100-nm thick with intermediate oxidation.

In the measurements, the sample was mounted in an aluminum alloy sample box which is fixed on the mixing chamber stage of a dilution refrigerator. The temperature of the mixing chamber was below 15 mK during measurements. The measurement setup is sketched in Fig. 1(b). The green circuit is used for applying the microwave to the $\lambda/4$ coplanar waveguide resonator, and the black circuit is used for applying the probe microwave. The red circuit is used for applying the DC bias to the DC superconducting quantum interference device (DC-SQUID). The probe signal is fed in via port 1 and attenuated to the single photon level when interacting with the Xmon qubit. The output signal is then amplified by an HEMT mounted at the 4 K stage before being sent to a room temperature microwave amplifier. The signal is finally detected by the microwave network analyzer.

In our experiment, we detect the energy level of the Xmon with the transmitted microwave spectrum.[31] Since the Xmon is a single artificial atom, a high probe power will saturate it; we thus reduce the probe power to detect the Xmon's scattering microwave signal. The experiment results are shown in Fig. 2(a). The data are measured with no driving of the resonator and zero DC bias to the qubit. We can see, as the probe power decreases, one peak appears at 6.369 GHz on the S_{21} spectrum, $S_{21} = V_{\text{out}}/V_{\text{in}}$.

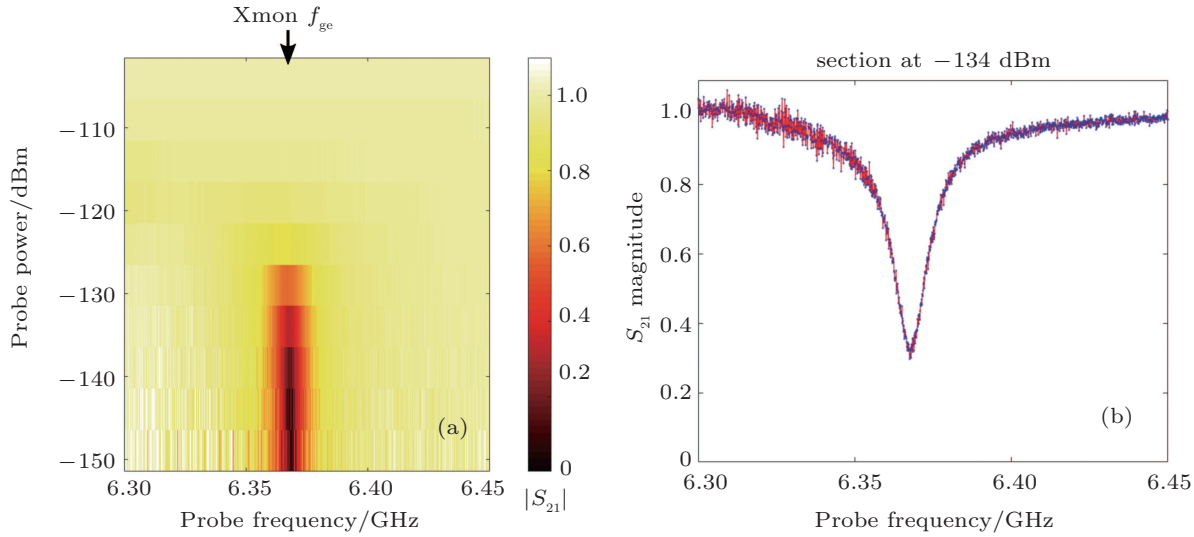


Fig. 2. (color online) (a) Measured S_{21} spectrum at different probe amplitude and frequency. The DC bias of the Xmon is set to 0 and there is no microwave field applied to the $\lambda/4$ coplanar waveguide resonator. A peak appears at f_{3LS}^{ge} while reducing the probe power. (b) S_{21} data of taken at a probe microwave at power of −134 dBm.

The whole two-dimensional energy spectrum of the qubit can be mapped out by changing the DC bias. The results are shown in Fig. 3(a). The inset in Fig. 3(a) shows the high resolution energy spectrum around the avoidcross, which corresponds to the degeneracy splitting while the resonator is in resonance coupling with the two lowest energy levels of the qubit, i.e., the transition frequency f_{3LS}^{ge} from ground $|g\rangle$ to first excited state $|e\rangle$ equals to the frequency of the resonator, $f_{3LS}^{ge} = f_r$. From the two-dimensional spectrum data shown in Fig. 3(a), it can be seen that the maximum of f_{3LS}^{ge} is 6.369 GHz, and the bare frequency of the $\lambda/4$ coplanar waveguide resonator is $f_r = 5.671$ GHz. In order to make the two upper levels of the qubit in resonance coupled with the $\lambda/4$ coplanar waveguide resonator, such that $f_{3LS}^{ef} = f_r$, the anharmonicity of the Xmon needs to be measured. Experimentally, the two-tone spectrometry is conducted to determine f_{3LS}^{ef}. The qubit is biased at the maximum frequency, while applying the pump microwave field at fixed frequency $f_{3LS}^{ge} = 6.369$ GHz, and sweeping a weak probe tone in the frequency. The weak probe field is used to detect the two upper levels of the qubit. The population of the first excited state $|e\rangle$ is increased due to the pump microwave, thus the spectra corresponds to the transition $|e\rangle \leftrightarrow |f\rangle$ that can be detected by the weak frequency-sweeping tone. From the spectrum data of the weak sweeping tone, it can be seen at this DC bias, $f_{3LS}^{ge} = 6.369$ GHz and $f_{3LS}^{ef} = 6.221$ GHz. The anharmonicity of the Xmon is $\Delta = f_{3LS}^{ef} - f_{3LS}^{ge} = -148$ MHz. In order to satisfy the resonance coupling condition $f_{3LS}^{ef} = f_r$, the Xmon needs to be adjusted to $f_{3LS}^{ef} = 5.671$ GHz, so the f_{3LS}^{ge} is estimated about 5.891 GHz. Also, from the two-dimensional spectrum, the DC bias value corresponding to this frequency can be found.

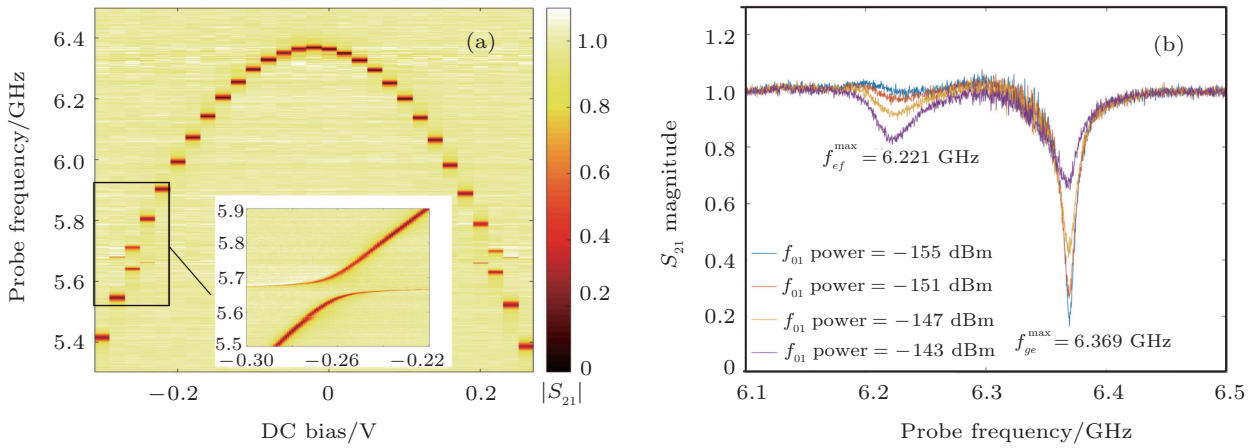


Fig. 3. (color online) (a) 2D energy spectrum of the Xmon qubit. The Xmon's f_{3LS}^{ge} as a function of DC bias is shown in this 2D S_{21} spectrum, and the inset is the avoidcross of the energy spectrum of the Xmon and resonator around $f_{3LS}^{ge} = f_r$. (b) Two-tone energy spectrum of the Xmon. The Xmon is biased at the maximum frequency point, a continuous microwave pump is applied at f_{3LS}^{ge} to the transmission line, and a weak frequency-sweeping probe is applied to detect the scattering spectrum of two upper levels of the qubit. As the pump power increases and the population of state $|e\rangle$ increases, the scattering signal of two upper levels $|e\rangle \leftrightarrow |f\rangle$ can be detected.

When the qubit is biased such that $f_{3LS}^{ef} = f_r$, the $\lambda/4$ coplanar waveguide resonator is resonantly coupled to the two upper levels of the qubit. The resonator is driven by a continuous microwave, and a low-power transmitted microwave signal around f_{3LS}^{ge} is applied to detect its S_{21} spectrum. When the $\lambda/4$ resonator is not driven, there is a single peak at f_{3LS}^{ge}, this peak correspond to $|g0\rangle \leftrightarrow |e0\rangle$ energy levels shown by the red transition in Fig. 4. As the driving power increases, the average photon number in the resonator is increased, the peak at f_{3LS}^{ge} weakens, two peaks appear beside f_{3LS}^{ge}, which corresponds to the blue transitions in Fig. 4.

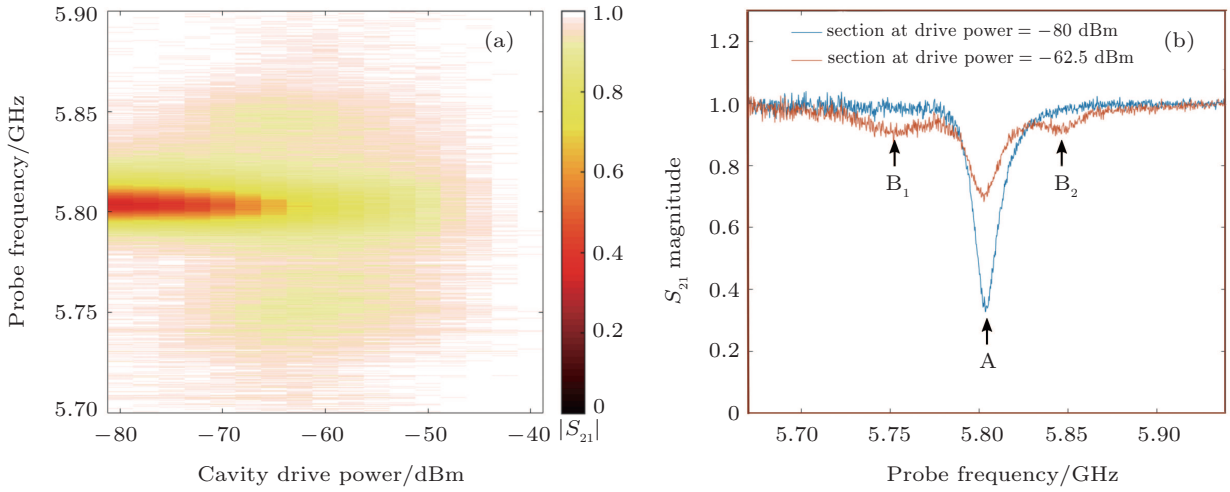


Fig. 4. (color online) (a) S_{21} measurement results with increasing driving field amplitude for the resonator. The Xmon is biased to satisfy the resonance condition that $f_{3LS}^{ef} = f_r$. Continuous microwave is applied to resonantly drive the $\lambda/4$ coplanar waveguide resonator, preparing it in the coherent state. Weak sweeping probe microwave is injected from port 1. As the driving power increases and the average number of photons in the resonator increases, the central peak at frequency f_{3LS}^{ge} weakens, and two side peaks appear beside the central peak. The central peak of the S_{21} spectrum corresponds to zero photon in the resonator , while the two side peaks correspond to one photon in the resonator. Because of the resonance coupling of the resonator and the two upper levels of Xmon, as shown in Fig. 5, there is an energy level splitting induced by this resonance single photon. (b) Spectrum section at different resonator driving power. There are three peaks while applying a strong enough microwave drive to the $\lambda/4$ coplanar waveguide resonator, and the middle peak corresponds to the transition between $|g0\rangle \leftrightarrow |e0\rangle$, labeled with red double arrows in Fig. 5, and the two side peaks besides the middle peak correspond to the blue transitions shown in Fig. 5.

3. Analysis and discussion

As mentioned previously, the cavity induced ATS has been reported for systems containing a flux qubit and a resonator. In that case, the ATS doublet peaks appear even when the input power to the cavity is zero. In other words, it is called vacuum induced ATS. In contrast, we do not observe such vacuum induced ATS.[26] We attributed this to the ladder-type energy level structure of our three-level quantum system, and the energy level diagram of the coupled system is shown in Fig. 5. When the cavity is in vacuum state $|0\rangle$ and average pho-

ton number $\langle n\rangle = 0$, the coupled system is in the ground state $|g0\rangle$. Thus, the transition between $|g0\rangle$ and $|e0\rangle$ can be probed, which is marked in Fig. 5 as transition A and corresponds to the spectrum peak A in Fig. 4(b). When driving the cavity to a coherent state with average photon $\langle n\rangle = 1$, the coupled system has a part of the population on $|g1\rangle$. Then the transition between $|g1\rangle$ to the $\alpha|e1\rangle + \beta|f0\rangle$ and $\alpha'|e1\rangle + \beta'|f0\rangle$ can also be detected, which are marked in Fig. 5 as transitions B1, B2 and correspond to spectrum peaks B1, B2 in Fig. 4(b). In this case, a triplet is shown. Continuously driving the cavity to the coherent state with average photon $\langle n\rangle > 1$, the population on $|g0\rangle$ reduces, then the transition A reduces, and spectrum peak A disappears.

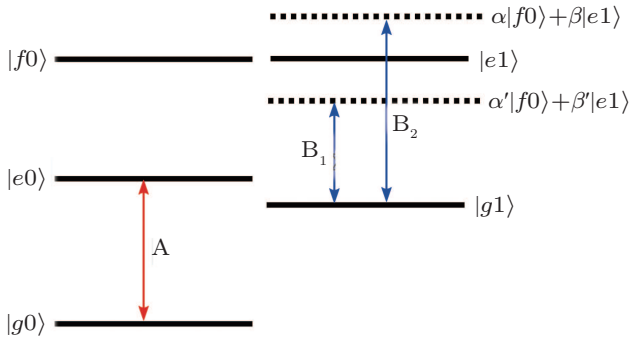


Fig. 5. (color online) The energy level diagram of the coupled system. The lowest three levels of Xmon are labeled with $|g\rangle$, $|e\rangle$, and $|f\rangle$, and the Fock state of the cavity is labeled with $|n\rangle, n \in [0,1,2,\ldots]$. The red transition corresponds to the state of zero photon in the resonator. The two blue transitions correspond to the state of one photon in the cavity, which is split by the resonance coupling between the resonator and two upper levels of the Xmon. This splitting is also known as degeneracy splitting of energy levels.

The two doublet peaks are 95 MHz apart and is about 47 MHz from the resonant central peak. According to the theoretical analysis in Ref. [26], the position of the two doublet peak with respect to the original resonant peak is equal to $\sqrt{2}g$,[28] where g is the coupling strength between the Xmon qubit and the resonator when there are a few photons in the resonator. The value of g can be obtained from the energy spectrum data in Fig. 3(a), in which the coupling between the qubit and the resonator results in a splitting at around 5.671 GHz. The splitting is $2g$. Thus, we can see that g is about 36 MHz. This value is approximately consistent with the ATS data shown in Fig. 1.

As discussed above, the observed ATS corresponded to the situation when the cavity average photon is around $\langle n\rangle = 1$. The theoretical analysis has suggested that the cavity induced ATS can resolve the photon number. This is due to the increased coupling strength that is proportional to $\sqrt{n}$, where n is the photon number. In other words, one would expect separate pairs of doublet peaks to appear when the average number of photons in the cavity is increased greater than one. However, the analysis presented in Ref. [26] suggests that the peak intensity is decreased progressively for an n value larger than one. The ATS doublet peaks, shown in Fig. 4(b), are already very weak. Thus, the other peaks could become too weak to be observed in our experiments.

One feature observed in our experiments is that the ATS peaks are not observed in the high power region. Theoretically, we would expect to see the ATS peaks move further apart as the power fed into the resonator is increased. It is not clear what causes this discrepancy. One possible reason is that the Xmon qubit has relatively small anharmonicity as compared to the flux qubit. In Ref. [27], cavity induce ATS is observed at the high power region. In fact, they observed a change in the regime of the Autler–Townes splitting from quantum (vacuum-induced) to classical (with many resonator photons).

4. Conclusion

We have investigated the Autler–Townes effect due to the quantized electromagnetic field on a superconducting quantum circuit that contains an Xmon qubit coupled to a transmission line and a $\lambda/4$ coplanar waveguide resonator. By performing transmission properties, we observed the qubit energy level spliting when the cavity is resonantly coupled to the two upper levels of the qubit. The average photon number in the cavity is believed to be around one. We propose that this type of superconducting quantum circuit could be used as a single photon switcher or router that are crucial elements in a quantum network.[13]

References

[1] Harris S E, Field J E and Imamoğlu A 1990 *Phys. Rev. Lett.* **64** 1107
[2] Harris S E, Field J E and Kasapi A 1992 *Phys. Rev. A* **46** R29
[3] Rice P R and Brecha R J 1996 *Opt. Commun.* **126** 230
[4] Gong Z R, Ian H, Zhou L and Sun C P 2008 *Phys. Rev. A* **78** 053806
[5] Nikoghosyan G and Fleischhauer M 2010 *Phys. Rev. Lett.* **105** 013601
[6] Giner L, Veissier L, Sparkes B, Sheremet A S, Nicolas A, Mishina O S, Scherman M, Burks S, Shomroni I, Kupriyanov D V, Lam P K, Giacobino E and Laurat J 2013 *Phys. Rev. A* **87** 013823
[7] Pei L, Lu X, Bai J, Miao X, Wang R, Wu L A, Ren S, Jiao Z, Zhu H, Fu P and Zuo Z 2013 *Phys. Rev. A* **87** 063822
[8] Peng B,Özdemir Ş K, Chen W, Nori F and Yang L 2014 *Nat. Commun.* **5** 5082
[9] Lu X, Miao X, Bai J, Pei L, Wang M, Gao Y, Wu L A, Fu P, Wang R and Zuo Z 2015 *J. Phys. B: At. Mol. Opt. Phys.* **48** 055003
[10] Autler S H and Townes C H 1955 *Phys. Rev.* **100** 703
[11] Anisimov P M, Dowling J P and Sanders B C 2011 *Phys. Rev. Lett.* **107** 163604
[12] Sun H C, Liu Y X, Ian H, You J Q, Il'ichev E and Nori F 2014 *Phys. Rev. A* **89** 063822
[13] Hoi I C, Wilson C M, Johansson G, Palomaki T, Peropadre B and Delsing P 2011 *Phys. Rev. Lett.* **107** 073601
[14] Ian H, Liu Y X and Nori F 2010 *Phys. Rev. A* **81** 063823
[15] Novikov S, Sweeney T, Robinson J E, Premaratne S P, Suri B, Wellstood F C and Palmer B S 2014 *Nat. Phys.* **12** 75
[16] Li H C, Ge G Q and Zhang H Y 2015 *Opt. Express* **23** 9844-9851
[17] Gu X, Huai S N, Nori F and Liu Y X 2016 *Phys. Rev. A* **93** 063827

[18] Liu Q C, Li T F, Luo X Q, Zhao H, Xiong W, Zhang Y S, Chen Z, Liu J S, Chen W, Nori F, Tsai J S and You J Q 2016 *Phys. Rev. A* **93** 053838
[19] Long J, Ku H S, Wu X, Gu X, Lake R E, Bal M, Liu Y X and Pappas D P 2018 *Phys. Rev. Lett.* **120** 083602
[20] Sillanpaa M A, Li J, Cicak K, Altomare F, Park J I, Simmonds R W, Paraoanu G S and Hakonen P J 2009 *Phys. Rev. Lett.* **103** 193601
[21] Baur M, Filipp S, Bianchetti R, Fink J M, Goppl M, Steffen L, Leek P J, Blais A and Wallraff A 2009 *Phys. Rev. Lett.* **102** 243602
[22] Abdumalikov A A Jr, Astafiev O, Zagoskin A M, Pashkin Y A, Nakamura Y and Tsai J S 2010 *Phys. Rev. Lett.* **104** 193601
[23] Suri B, Keane Z K, Ruskov R, Bishop L S, Tahan C, Novikov S, Robinson J E, Wellstood F C and Palmer B S 2013 *New J. Phys.* **15** 125007
[24] Novikov S, Robinson J E, Keane Z K, Suri B, Wellstood F C and Palmer B S 2013 *Phys. Rev. B* **88** 060503
[25] Tanji-Suzuki H, Chen W, Landig R, Simon J and Vuletic V 2011 *Science* **333** 1266
[26] Ding J H, Huai S N, Ian H and Liu Y X 2017 arXiv: 1707 02707 [quant-ph]
[27] Peng Z H, Ding J H, Zhou Y, Ying L L, Wang Z, Zhou L, Kuang L M, Liu Y X, Astafiev O and Tsai J S 2017 arXiv: 1705 11118 [cond-mat physics:quant-ph]
[28] Koch J, Yu T M, Gambetta J, Houck A A, Schuster D I, Majer J, Blais A, Devoret M H, Girvin S M and Schoelkopf R J 2007 *Phys. Rev. A* **76** 042319
[29] Barends R, Kelly J, Megrant A, et al. 2013 *Phys. Rev. Lett.* **111** 080502
[30] Kelly J S 2015 "Fault-tolerant superconducting qubits", Ph. D. Dissertation (Santa Barbara: University of California)
[31] Astafiev O, Zagoskin A M, Abdumalikov A A, Pashkin Y A, Yamamoto T, Inomata K, Nakamura Y and Tsai J S 2010 *Science* **327** 840